Published in final edited form as:

*Nat Genet*. ; 44(6): 714–719. doi:10.1038/ng.2277.

# CCDC103 mutations cause primary ciliary dyskinesia by disrupting assembly of ciliary dynein arms

**Jennifer R. Panizzi**[1,2,*], **Anita Becker-Heck**[3,4,*], **Victoria H. Castleman**[5], **Dalal Al-Mutairi**[6], **Yan Liu**[1], **Niki T. Loges**[4], **Narendra Pathak**[1,2], **Christina Austin-Tse**[7], **Eamonn Sheridan**[6], **Miriam Schmidts**[5], **Heike Olbrich**[4], **Claudius Werner**[4], **Karsten Häffner**[3], **Nathan Hellman**[1,2], **Rahul Chodhari**[8], **Amar Gupta**[1], **Albrecht Kramer-Zucker**[9], **Felix Olale**[10], **Rebecca D. Burdine**[11], **Alexander F. Schier**[12], **Christopher O'Callaghan**[13], **Eddie MK Chung**[8], **Richard Reinhardt**[14], **Hannah M. Mitchison**[5,14], **Stephen M. King**[15,#], **Heymut Omran**[4,#], and **Iain A. Drummond**[1,2,7,#]

[1]Nephrology Division, Massachusetts General Hospital, Charlestown, MA, USA [2]Department of Medicine, Harvard Medical School, Boston, MA, USA [3]University Hospital Freiburg, Freiburg, Germany [4]Klinik und Poliklinik fuer Kinder- und Jugendmedizin -Allgemeine Paediatrie-, Universitätsklinikum Münster, Münster, Germany [5]Molecular Medicine Unit, University College London, Institute of Child Health, London, UK [6]Leeds Institute of Molecular Medicine, Wellcome Trust Brenner Building, St James's University Hospital, Leeds, UK [7]Department of Genetics, Harvard Medical School, Boston, MA, USA [8]General and Adolescent Paediatrics Unit, University College London, Institute of Child Health, London, UK [9]Renal Division, University Hospital Freiburg, Freiburg, Germany [10]Skirball Institute of Biomolecular Medicine, New York University School of Medicine, New York, NY, USA [11]Department of Molecular Biology, Princeton University, Princeton, New Jersey, USA [12]Department of Molecular and Cellular Biology, Harvard University, Cambridge, MA, USA [13]Department of Infection, Immunity, and Inflammation, University of Leicester, Leicester, England [14]Genome Centre Cologne at MPI for Plant Breeding Research,



[#]Corresponding Authors: Iain Drummond, Nephrology Division, MGH, 149 13th Street, Charlestown, MA 02129, 617 726 5647, idrummon@receptor.mgh.harvard.edu. Heymut Omran, Universitätsklinikum Münster, - Klinik und Poliklinik für Allgemeine, Kinder- und Jugendmedizin, Albert-Schweitzer-Campus 1, 48149 Münster, Tel.: +49 (251) 83 477 32, heymut.omran@ukmuenster.de. Stephen M. King, Department of Molecular, Microbial and Structural Biology, University of Connecticut Health Center, 263 Farmington Avenue, Farmington, CT 06030-3305, 860 679 3347, king@neuron.uchc.edu.
[*]These authors contributed equally

**Accession numbers**

The zebrafish *ccdc103* full-length wild-type gene coding sequence corresponds to GenBank record NM_001002753. Human CCDC103: NM_213607. Chlamydomonas: AV626473.

**Author Contributions.** Genetic mapping and Ccdc103/CCDC103 characterization in zebrafish were conducted by J.R.P., Y.L., C.A-T., A.G. N.H., A.K.Z., R.B., F.O., A.F.S., N.P. and I.A.D. Studies with patient samples were conducted by A.B.-H.,D.A., N.T.L., E.S., M.S., H.O., C.W., K.H., R.C., C.C., E.M.K.C, R.R., H.M.M. and H.O. *Chlamydomonas* studies were performed by S.K.. The manuscript was prepared by J.R.P., A.B.-H., S.K., H.O. and I.A.D.

The authors state that they have no competing financial interests.

**URLs**

Polyphen-2 software analysis: http://genetics.bwh.harvard.edu/pph2
dbSNP: http://www.ncbi.nlm.nih.gov/projects/SNP/
dbSNP human polymorphism database: http://www.ncbi.nlm.nih.gov/projects/SNP/
1000 Genomes Project human polymorphism database: http://www.1000genomes.org/
NHLBI-ESP human polymorphism database: http://evs.gs.washington.edu/EVS/

Köln, Germany [15]Department of Molecular, Microbial and Structural Biology, University of Connecticut Health Center, Farmington, CT, USA

## Abstract

Cilia are essential for fertilization, respiratory clearance, cerebrospinal fluid circulation, and to establish laterality[1]. Cilia motility defects cause Primary Ciliary Dyskinesia (PCD, MIM 242650), a disorder affecting 1:15-30,000 births. Cilia motility requires the assembly of multisubunit dynein arms that drive cilia bending[2]. Despite progress in understanding the genetic basis of PCD, mutations remain to be identified for several PCD linked loci[3]. Here we show that the zebrafish cilia paralysis mutant *schmalhans*$^{tn222}$ *(smh)* mutant encodes the coiled-coil domain containing 103 protein (Ccdc103), a *foxj1a* regulated gene. Screening 146 unrelated PCD families identified patients in six families with reduced outer dynein arms, carrying mutations in *CCDC103*. Dynein arm assembly in *smh* mutant zebrafish was rescued by wild-type but not mutant human CCDC103. Chlamydomonas Ccdc103 functions as a tightly bound, axoneme-associated protein. The results identify Ccdc103 as a novel dynein arm attachment factor that when mutated causes Primary Ciliary Dyskinesia.

Zebrafish *schmalhans* (*smh*$^{tn222}$) mutants[4] exhibit curved body axis, randomized left-right asymmetry, and pronephric kidney cysts (figure 1A-B and Supplementary Table 1), characteristic features of ciliopathy[5]. Electron microscopy of *smh*$^{tn222}$ cilia revealed that compared to wildtype cilia (figure 1C), *schmalhans* mutant cilia completely lacked inner and outer dynein arms (figure 1D and Supplementary figure 1), while cilia length was not altered (Supplementary figure 2). High-speed microvideo and linescan analysis of wildtype zebrafish pronephric cilia (figure 1E; Supplementary Movie 1) or olfactory placode multicilia (Supplementary figure 3; Supplementary Movie 2) revealed rhythmic cilia motility. However, consistent with dynein arm defects, *schmalhans* mutant cilia were completely paralyzed in the pronephros (figure 1F; Supplementary Movie 3), the olfactory placode (Supplementary figure 3 B,D; Supplementary Movie 4), and in the spinal canal (Supplementary movies 5 and 6). The *schmalhans* $^{tn222}$ mutation was mapped to a ~2Mb region of Chromosome 3 and subsequently fine mapped to a 0.43Mb region containing 8 genes (Supplementary figure 4 and Supplementary Tables 2 and 3). Sequencing candidate genes in this interval revealed a C>T mutation at nucleotide 79 in exon 1 of *zgc:100838 (ccdc103)*, generating a predicted Q>Stop at amino acid 27 of the 247 amino acid protein (Dr-Q27Stop) (Figure 1G,H). Embryo injection of myc-tagged wild-type *ccdc103* mRNA rescued axis curvature, left-right asymmetry defects, and kidney cyst phenotypes, and also restored cilia motility in *smh* mutants (figure 1I,J; Supplementary Movie 7 and data not shown), confirming that *ccdc103* was the *schmalhans* mutant gene. Mutant Ccdc103 mRNA carrying the Q27Stop *smh* mutation not only failed to rescue but also increased the frequency of axis curvature defects, suggesting it may act as a dominant-negative (figure 1K). Antisense morpholino knockdown of *ccdc103* induced curved body axes, left-right asymmetry defects, hydrocephalus, and kidney cysts (Supplementary figure 5 A,B and Supplementary Table 4), and caused cilia paralysis (Supplementary Movie 8), phenocopying

*schmalhans*. Together, these data identify *ccdc103* as an essential gene for dynein arm assembly and cilia motility.

Whole genome linkage analysis in a group of four consanguineous Pakistani PCD families from a UK-based genetic isolate[6] with absent inner and outer dynein arms revealed a novel PCD locus on chromosome 17q12-q22 containing the human *ccdc103* ortholog, *CCDC103*. The maximum HLOD score was 4.8 with an α value (proportion of linked families) of 1. The critical genetic interval spanned 14 cM (16 Mb) between SNP markers *rs1859212* and *rs2045418* (Supplementary figure 6). Screening affected individuals of the Pakistani PCD families as well as nine other Pakistani patients with identified linkage to *CCDC103* and 132 unrelated PCD families (54% ODA defects; 47% functional or other structural PCD defects) for mutations in *CCDC103* identified ten PCD patients carrying DNA exchanges in the *CCDC103* (NM_213607) coding sequence (figure 2, Supplementary figure 7,8). We found homozygous loss-of-function mutations in three chromosome 17-linked Pakistani families (UCL120, OP-1192 and OP-1193) with six affected individuals (c.383_384insG) predicting a frame shift and premature termination of translation (p.Gly128fs25*) (figure 2, Supplementary figure 7). The three families originate from nearby regions in Pakistan making it very likely that the mutations result from a common founder (ancestor). The consanguineous parents of family UCL120 and OP-1193 were heterozygous for this truncating mutation (figure 2), consistent with autosomal recessive inheritance and homozygosity by descent. In two other chromosome 17-linked Pakistani families (Supplementary figure 8; UCL143 and OP-1194) and a German family (Supplementary figure 8; OP-32), we identified in all four affected individuals (OP-31II1, OP-31II2, UCL-143II1; OP-1194II1) a homozygous transversion (c.A461C) that converts a histidine to a proline at amino acid 154 (p.His154Pro) that co-segregated with the disease phenotype (Supplementary figure 8). Multiple sequence alignment (Supplementary figure 9) showed that the p.His154Pro exchange occurred in a region flanking a highly conserved domain of Ccdc103. Polyphen-2 software analysis generated a protein damage score of 0.972 for this mutation, highly suggestive of pathogenic significance. The c.A461C variant was absent in 180 Caucasian controls as well as in the dbSNP, 1000 Genomes Project and NHLBI-ESP human polymorphism databases. Eight other UK-Pakistani families compatible with linkage to the *CCDC103* locus (Supplementary figure 6 for UCL130, UCL145) did not carry mutations in *CCDC103* coding sequences. In one other family, an affected child carried a heterozygous transversion (c.G31C) predicting an alanine to proline change (p.Ala11Pro) with no mutation on the other allele.

All six affected individuals carrying recessive truncating *CCDC103* mutations exhibited typical clinical findings for PCD (Supplementary Table 5) comprising recurrent upper and lower airway infections, sinusitis and documented lung damage (bronchiectasis), and two affected displayed dextrocardia and one *situs inversus*. In four other PCD affected individuals we identified homozygous amino-acid exchange p.His154Pro. Two patients had *situs inversus totalis*, one had situs inversus abdominalis, one dextrocardia and one exhibited normal organ situs. Our findings indicate that *CCDC103* mutations cause PCD and randomization of left/right body asymmetry resembling findings in *smh* mutant zebrafish.

To test the pathogenic significance of the identified *CCDC103* variants (figure 3A), we assayed their function in zebrafish *smh* mRNA rescue experiments. Injection of myc-tagged wildtype human *CCDC103* mRNA completely rescued the *smh* mutant phenotype (Figure 3B,C). mRNA encoding the *CCDC103* Hs-Ala11Pro variant also completely rescued the *smh* mutant phenotype (Figure 3B,C) confirming that the heterozygous p.Ala11Pro variant observed in one PCD individual represents a rare, nonpathogenic polymorphism. mRNAs encoding the p.His154Pro and p.Gly128fs25* variants failed to fully rescue the *smh* axis curvature or cilia motility phenotypes, indicating that these mutations are pathogenic (Figure 3B,C; Supplementary Table 6,7). Notably, expression of *CCDC103* p.His154Pro partially rescued the *smh* body axis curvature; 13 of 27 Hs-His154Pro mRNA-injected, homozygous mutants by genotype displayed a mild “bent” phenotype and lacked full curvature (Figure 3B, Supplementary Table 6), indicating that the Hs-His154Pro variant may represent a hypomorphic mutation. Wildtype epitope-tagged CCDC103 protein migrated as a monomer and dimer in denaturing SDS gels with a major band at approximately 56 KD and a minor band at 27.6 KD (Figure 3D), the predicted size of the CCDC103 monomer. While the mRNA encoding the rescuing CCDC103 p.Ala11Pro protein (M2; figure 3D) was expressed similarly to wildtype, mutant CCDC103 proteins that failed to rescue *smh* embryos were unstable in vivo and did not generate significant amounts of protein (p.His154Pro; M1 and p.Gly128fs25*; M3, figure 3D) even when injected at ten-fold higher doses (350 pg; data not shown). Consistent with its ability to rescue *smh* mutant phenotypes, wild-type human *CCDC103* mRNA also restored dynein arms to genotypically mutant axonemes (figure 3E).

Defects in ODA composition in human axonemes were analysed by immunofluorescence microscopy of respiratory cells. Cells of patient OP-1192II1 carrying the homozygous p.Gly128fs25* loss-of-function mutation demonstrated partial loss of ODA complexes along the ciliary axonemes (Figure 4A–C) with some proximally localized type 1 ODA complexcomponents DNAH5 and DNAI2 still present in the ciliary axonemes. In contrast, DNAH5 and DNAI2 were absent from the distal ciliary axonemes with DNAH5 accumulating in the perinuclear and apical cytoplasm (figure 4A). This is consistent with absence of distally localized type-2 ODA complexes, which we confirmed by absence of DNAH9 from the ciliary axonemes in mutant cilia (figure 4C). This defect is very similar to findings obtained in patients carrying mutations in the dynein arm assembly factor KTU[7]. In addition we analyzed respiratory cells from the PCD patient OP-1194II1 carrying the homozygous hypomorphic p.His154Pro variant. The mutant cells displayed a normal localization of DNAH5, DNAI2 and DNAH9 (data not shown). Interestingly, both patients showed normal localization of the IDA component DNALI1 (data not shown), thus at least parts of IDA components can be assembled in the ciliary axoneme. TEM analysis of all three affected individuals of the UCL-120 family harboring the homozygous *CCDC103* p.Gly128fs25* loss-of-function mutation showed either loss or strong reduction in outer dynein arms (shown for UCL-120II2 and UCL-120II3; figure 4D), similar to the *smh* mutant phenotype (figure 1D). Variation in the degree of the ODA defects in the three affected UCL-120 siblings (figure 4D) may reflect the position (proximal vs. distal) of the cilia cross section since some proximal ODA components can persist in *CCDC103* p.Gly128fs25* mutant cilia (figure 4A,B). The effects of *CCDC103* mutations were further analysed by high-speed videomicroscopy of respiratory cells obtained by nasal brushing biopsy. Normal

respiratory cell cilia beat vigorously and coordinately (Supplementary Movie 9). Consistent with severe outer dynein arm defects observed by EM (figure 4D), patients carrying the homozygous p.Gly128fs25* mutation (OP-1193 II1) exhibited complete cilia paralysis (Supplementary Movie 10). Patients carrying the homozygous p.His154Pro mutation exhibited either reduced cilia beat amplitude (patient OP-32II1; Supplementary Movie 11) or loss of beat coordination and cilia paralysis (patient OP-32II2; Supplementary Movie 12; compare with control Supplementary Movie 13), consistent with the variable reduction in EM ODA arm structure in these patients which ranged from apparently normal to complete ODA/IDA loss (patient UCL-143II1; Supplementary figure 10). The less severe phenotype seen in affected children of family OP-32 is consistent with our CCDC103 functional assays in zebrafish that identified the p.His154Pro exchange as a hypomorphic mutation. The variable phenotype observed within the UCL-120 family and among affected children of different families harboring identical mutations (UCL-143; OP-32) may suggest modulation of the phenotype by genetic modifiers frequently observed in ciliopathies[8].

*ccdc103* mRNA was highly expressed in all zebrafish cells bearing motile cilia (Supplementary figure 11) and was not expressed in *foxj1a*-deficient embryos (Supplementary figure 11), indicating that *ccdc103* expression is controlled coordinately with *foxj1* motile cilia target genes[9]. Ccdc103 protein was expressed both in the cytoplasm and axonemes of zebrafish olfactory placode cells (figure 5A); Ccdc103 staining was not observed in *smh* morpholino knockdown embryos (Supplementary figure 12). To gain insight into the function of Ccdc103 in dynein arm assembly we examined the *Chlamydomonas ccdc103* ortholog, Pr46b (Supplementary figure 9). Like zebrafish Ccdc103, Pr46b protein was present in both flagella and cytoplasmic extracts and migrated as apparent monomers and dimers on SDS gels (figure 5B,C), similar to protein expressed in zebrafish embryos (figure 3G). In isolated flagella, Ccdc103/Pr46b was tightly associated with axonemes even after 0.6 M NaCl extraction (figure 5B). Fractionation of *Chlamydomonas* cytoplasm (Figure 5C) identified Ccdc103/Pr46b in high molecular weight complexes (440 KD - 2 MD) that co-purified with outer arm dynein light chain LC2, as well as in lower molecular weight complexes (<440,000 Da). Analysis of human CCDC103 expression in respiratory epithelial cells confirmed that CCDC103 is present as apparent monomers and dimers (Supplementary figure 13 B,C). The remarkable stability of putative dimeric forms of Ccdc103 protein in heat-denatured, SDS gel samples prompted us to further examine the properties of recombinant Ccdc103/Pr46b protein. Circular dichroism spectroscopic analysis of Ccdc103/Pr46b revealed a high alpha helical content, and thermal titration (temperature range 4–85° C) showed that Ccdc103 was remarkably thermo-stable since it was not fully denatured even at 85° C (figure 5D). Furthermore, the helical content of ccdc103/Pr46b was not diminished by addition of 1% SDS and heating at 100° C for 2.5 minutes (Supplementary figure 14). Gel filtration of purified Ccdc103/Pr46b protein revealed peaks corresponding to a mixture of monomeric and dimeric forms of Ccdc103/Pr46b (figure 5E, Supplementary figure 15), confirming that Ccdc103 can homodimerize. Thus, the stability of Ccdc103 dimers during SDS gel electrophoresis is due to the extraordinary thermal tolerance of the protein. We noted previously that over-expression of *smh* mutant Q27Stop Ccdc103 protein containing part of the N-terminal coiled-coil domain could have dominant effects in zebrafish embryos and induce ciliopathy phenotypes (figure

1K). To test whether *smh* mutant Ccdc103 might exert these effects by interfering with wild-type Ccdc103 dimer formation, full-length myc-tagged Ccdc103 and *smh* N-terminal Q27Stop mRNAs were co-expressed in zebrafish embryos. Increasing amounts of N-terminal Q27Stop Ccdc103 reduced the Ccdc103 dimer : monomer ratio (figure 5F), linking Ccdc103 function to homodimer formation. Finally, Ccdc103/Pr46b protein remained stably associated with axonemes in mutants lacking other dynein arm components including ODA docking complex proteins (Supplementary figure 16). This, along with its stable association with axonemes in high salt (figure 5B) distinquishes Ccdc103 from the docking complex proteins[10–12] and indicates it is a core factor for dynein arm binding to cilia microtubules. Taken together, our findings demonstrate an essential role for Ccdc103 as a novel coiled-coil containing, *foxj1a*-regulated dynein arm anchoring factor required for cilia motility. Although the patient families examined in this work showed typical recessive PCD, ciliopathy induced by over expression of the *ccdc103/schmalhans* mutant protein raises the possibility that dominant mutations could also contribute PCD. Future studies should reveal how Ccdc103 assembles with other ODA proteins[10–12] to ultimately anchor dynein motor complexes to cilia microtubules.

## Methods

### Zebrafish maintenance, embryo generation, and staging

Wild-type (WT) zebrafish of AB, TUAB, TL, and hybrid strains were maintained as previously described[13]. Embryos were obtained from natural matings, kept at 28.5°C in E3 solution with or without 0.003% 1-Phenyl-2-thiourea (PTU, Sigma) to suppress pigmentation, and staged according to morphology and/or age, as indicated[14].

### Positional cloning of the mutant locus

A genomic DNA panel was isolated from 1200 homozygous mutant zebrafish embryos of a heterozygous mating, along with genomic DNA from siblings, using Lysis buffer (10mM Tris-Cl, pH 8.3, 50 mM KCl, 0.3% Tween20, 0.3% Nonidet P40, 0.5 μg/μl Proteinase K). SSRP analysis was conducted by PCR amplification of markers followed by 6% polyacrylamide gel electrophoresis and staining with SYBR gold in 0.5xTBE. Zebrafish SNPs were identified using Ensembl browser, then PCR amplified and sequenced (Massachusetts General Hospital DNA Core).

### Cloning of *ccdc103*

Total RNA was isolated from 48-hour WT zebrafish embryos with TRIzol Reagent (Invitrogen), and used to produce cDNA via Superscript First-Strand Synthesis (Invitrogen). Using *zf-ccdc103* RT primers (Supplementary Table 2), zebrafish *ccdc103* was PCR-amplified with Platinum Pfx DNA Polymerase (Invitrogen) to incorporate Gateway cloning sites. The complete coding sequence was cloned into pDONR221 (Invitrogen), then pCS2+ vector[15] modified for Gateway cloning and verified by sequencing. N-terminal tagged *ccdc103* constructs were made by subcloning into Gateway-myc-pCS2+ (gift from Dr. N. Lawson, U. Mass, Worcester). Human *CCDC103* was cloned in the same manner, except it was PCR-amplified from Open Biosystems clone 5455678 (Genbank BC041060) using h-CCDC103 RT primers (Supplementary Table 2). The zebrafish *ccdc103* full-length wild-

type gene coding sequence reported in this paper corresponds to the existing GenBank record NM_001002753.

For genotyping embryos, genomic DNA was isolated as described above with Lysis buffer, then a 436 bp fragment spanning the mutation point was PCR amplified with *smh* genotyping primers (Supplementary Table 2). The fragment was digested with BfaI (New England Biolabs, NEB), a restriction site introduced by the *smh* mutation. Mutant DNA was cut into fragments of 351 and 85 bp, which were separated by agarose gel electrophoresis. When necessary, these results were verified by DNA sequencing.

## In situ hybridization

Sense and antisense probes for *ccdc103* were made from a pCRII construct of 1329 bp containing some 3' UTR sequence made by TOPO-TA cloning (Invitrogen) after amplification from cDNA with *zf-ccdc103 in situ* primers (Supplementary Table 2). Probes were synthesized with digoxigenin NTPs (Roche) after template linearization with BamHI (sense) or XbaI (anti-sense) before RNA synthesis with T7 or SP6 RNA polymerases, respectively. Embryos were fixed at the indicated stages and processed essentially as previously-described[16]. Antisense probes for *cardiac myosin light chain 2* (*myl7*)[17], *preproinsulin* (*ins*)[18], *foxa3*[19], and *pitx2*[20], were prepared as described previously.

## RNA and morpholino injections

Capped sense RNA encoding Ccdc103 was synthesized with SP6 RNA polymerase (Ambion mMessage mMachine) after linearization of pCS2-*ccdc103* with NotI. RNA was purified using G-50 Sephadex Quick Spin Columns (Roche) and diluted to the indicated concentrations with tissue culture grade distilled water. Microinjections were performed on 1–4 cell embryos using a Nanoliter 2000 (World Precision Instruments, Inc.)

A translation-blocking morpholino oligonucleotide (MO), $MO^{AUG}$ (Supplementary Table 2; Gene-Tools, LLC) targeted to the 5'-UTR, and a splice-blocking MO, $MO^{SPL}$ (Supplementary Table 2; Gene-Tools, LLC) targeted to the exon 2/intron 2 boundary were resuspended in DEPC treated water to stock concentrations of 20 μg/μl then further diluted to the given concentrations with DEPC water prior to injection.

*foxj1a* morpholino injections were performed using a cocktail of splice-and translation-blocking oligonucleotides, as previously described[21].

## Protein expression and antibody production

**Zebrafish—**Full-length zebrafish Ccdc103 coding region was subcloned and expressed using the Champion pET160 Gateway Expression System (Invitrogen). The protein was purified from cell insoluble fractions after resuspension in 3M NaSCN, then purified using His-Trap HP affinity columns (GE Healthcare) with imidazole gradient elution. Purified protein was dialyzed overnight into PBS, and sent to Rockland Immunochemicals for guinea pig polyclonal antibody production. Antibody was purified separately from serum of two animals by affinity purification on a Ccdc103 column prepared using AminoLink Plus Immobilization Kit (Thermo Scientific).

**Chlamydomonas—**The 70–267 residue region of *Chlamydomonas* Ccdc103/Pr46b was obtained by PCR from EST clone AV626473 and subcloned into pMal-c2 vector (NEB). The complete fusion protein was used for production of rabbit antibody CT285 (Covance Immunology Services, Denver, PA). Specific antibody was obtained by blot purification against recombinant Ccdc103/Pr46b (residues 70–267).

## Western blotting

Western blotting on embryo extracts was performed as previously described[22] using Rabbit anti-c-myc at 1:10000 and Goat anti-rabbit-HRP at 1:5000, or 1:2000 mouse anti-alpha tubulin and 1:4000 goat anti-mouse-HRP.

## Immunofluorescence Analysis

**Zebrafish—**Embryos were fixed with Dent's fixative (20%DMSO/80%Methanol) overnight, then washed in phosphate buffered saline plus 0.1%Tween20 (PBST) before incubation in blocking solution (5% Goat serum/5mg/ml bovine serum albumin/2%DMSO). Prior to blocking embryos for anti-zCcdc103 staining, they were incubated in 6M urea/0.1M glycine at 4C for 10 minutes. After blocking, primary antibodies were added in block solution overnight at 4C. Guinea pig anti-zCcdc103 was used at 1:100 dilution, while mouse anti-acetylated tubulin (Sigma) was used at 1:1000. Embryos were washed with PBST then secondary antibodies were added in block solution for 2 hours at room temperature. CY3-conjugated anti-guinea pig secondary antibodies (Jackson ImmunoResearch Laboratories, Inc.) were used at 1:200, while Alex488 or Alexa546 anti-mouse antibodies (Invitrogen) were used at 1:1000. After washing in PBST, embryos were analyzed by confocal microscopy (Zeiss LSM 5 Pascal) using a 63X oil immersion lens. Confocal stacks were deconvolved using Huygens Universal software and rotated to desired position prior to acquiring single frame images.

**Human—**Respiratory epithelial cells were obtained by nasal brush biopsy (Engelbrecht Medicine and Laboratory Technology, Germany) and suspended in cell culture medium. Samples were spread onto glass slides, air dried and stored at −80°C until use. Cells were treated with 4% paraformaldehyde, 0.2% Triton-X 100 and 1% skim milk prior to incubation with primary (at least 3 hours at room temperature or overnight at 4°C) and secondary antibodies (30 minutes at room temperature) . Controls were performed omitting the primary antibodies. Monoclonal anti-DNALI1 antibody and monoclonal anti-DNAH5 were reported previously[7,23]. Polyclonal rabbit anti-α/β-tubulin was used from Cell Signaling Technology (USA). Highly cross-adsorbed secondary antibodies (Alexa Fluor 488, Alexa Fluor 546) were obtained from Molecular Probes (Invitrogen). DNA was stained with Hoechst 33342 (Sigma). Confocal images were taken on a Zeiss LSM 510 I-UV.

## Patients and families

Signed and informed consent was obtained from patients fulfilling diagnostic criteria of PCD[3] and family members using protocols approved by the Institutional Ethics Review Board at the University of Freiburg, University College London Hospital NHS Trust, and collaborating institutions. We studied DNA from a total of 144 PCD patients originating from 141 unrelated families.

### Human linkage analysis

For whole genome linkage analysis, family samples were analysed using the Illumina SNP-based Linkage IVb Panel consisting of 6,008 evenly spaced SNPs with an average density of 0.64 cM. Standard parametric multipoint linkage analysis was carried out using MERLIN 1.0.1 software assuming autosomal recessive inheritance, a disease allele frequency of 0.007 and a disease penetrance of 0.9.

### Transmission electron microscopy

Zebrafish embryos were prepared for TEM by previously published protocols[24]. Human biopsies were prepared for TEM as previously reported[25].

### High-speed video analyses of ciliary beat

**Human cells—**Ciliary beat was assessed with the SAVA system. Trans nasal brush biopsies were rinsed in cell culture medium and immediately viewed with an Olympus IMT-2 inverted phase-contrast microscope equipped with a Redlake ES-310 Turbo monochrome high-speed video camera (Redlake, San Diego, USA) and a 40x objective. Digital image sampling was performed at 125 frames per second and 640x480 pixel resolution. The ciliary beat pattern was evaluated by slow motion playback (30 fps).

**Zebrafish—**Movies of olfactory, pronephric duct, and spinal canal cilia from 52 hpf embryos were captured at 240 frames per second using a 40X water immersion lens on Nikon Eclipse E800 with DragonFly Express high-speed camera (Point Grey Research, Inc.) and processed as described[26] for viewing at 15 fps.

### *Chlamydomonas* Strains

Strains used in this study were obtained from the *Chlamydomonas* Center and grown as described[27].

### *Chlamydomonas* fractionation

Cells were harvested by centrifugation, deflagellated using dibucaine and flagella isolated by standard methods[28]. Cell bodies were disrupted using an Emusiflex-C3 cell disruptor, clarified by centrifugation and concentrated using an Amicon Ultra 4 ultrafiltration unit (10,000 Da cutoff). Extract was fractionated in a Superose 6 10/300 GL column equilibrated with 20 mM Tris.Cl pH8.0, 0.5 mM EDTA, 5 mM $MgSO_4$, 150 mM NaCl. The column was calibrated with blue dextran (>$2\times10^6$ Da) and ferritin (440,000 Da), and 0.5 ml fractions were collected. Samples were electrophoresed in 10% SDS polyacrylamide gels and either stained with Coomassie blue or blotted to nitrocellulose and probed with antibody CT285. Immunoreactive bands were detected by chemiluminescence using an ImageQuant LAS4000 digital imaging system.

### Recombinant Protein Analysis

Soluble recombinant His10-tagged Ccdc103/Pr46b was purified by nickel chromatography. After removal of the tag by cleavage with Factor Xa, protein was analyzed by gel filtration

using Superose 6 and Superdex 200 columns. Circular dichroism spectroscopy was performed using a Jasco J-715 spectropolarimeter.

## Supplementary Material

Refer to Web version on PubMed Central for supplementary material.

## Acknowledgments

We wish to thank the patients and their families for their participation, and acknowledge support from the PCD Family Support Group (UK) and the German patient support group “Kartagener Syndrom und Primaere Ciliaere Dyskinesie e.V.”. We thank Professor R. Mark Gardiner and Dr Eduardo Moya for their help and involvement in the study. We thank Robert Hirst, Andrew Rutman for electron microscopy. We thank Angelina Heer, Christian Warmt, Denise Nergenau, Ramila S. Patel-King and Li Luo for excellent technical assistance. This work was funded by NIH grants DK053093 (I.A.D), GM051293 (S.M.K.), NRSA fellowship grant F32DK083868 (J.R.P), an American Heart Association Established Investigator Award to A.F.S.; DFG grants (DFG Om 6/4, GRK1109, SFB592), EU-grant SYSCILIA, and kindness for kids grant to H.O. The Medical Research Council UK, the Wellcome Trust and the Fondation Milena Carvajal Pro-Kartagener.

## References cited

1. Sharma N, Berbari NF, Yoder BK. Ciliary dysfunction in developmental abnormalities and diseases. Curr Top Dev Biol. 2008; 85:371–427. [PubMed: 19147012]
2. Satir P, Christensen ST. Overview of structure and function of mammalian cilia. Annu Rev Physiol. 2007; 69:377–400. [PubMed: 17009929]
3. Zariwala MA, Knowles MR, Omran H. Genetic defects in ciliary structure and function. Annu Rev Physiol. 2007; 69:423–50. [PubMed: 17059358]
4. Brand M, et al. Mutations affecting development of the midline and general body shape during zebrafish embryogenesis. Development. 1996; 123:129–42. [PubMed: 9007235]
5. Wessely O, Obara T. Fish and frogs: models for vertebrate cilia signaling. Front Biosci. 2008; 13:1866–80. [PubMed: 17981674]
6. O'Callaghan C, Chetcuti P, Moya E. High prevalence of primary ciliary dyskinesia in a British Asian population. Arch Dis Child. 2010; 95:51–2. [PubMed: 19720631]
7. Omran H, et al. Ktu/PF13 is required for cytoplasmic pre-assembly of axonemal dyneins. Nature. 2008; 456:611–6. [PubMed: 19052621]
8. Stoetzel C, et al. BBS10 encodes a vertebrate-specific chaperonin-like protein and is a major BBS locus. Nat Genet. 2006; 38:521–4. [PubMed: 16582908]
9. Yu X, Ng CP, Habacher H, Roy S. Foxj1 transcription factors are master regulators of the motile ciliogenic program. Nat Genet. 2008; 40:1445–53. [PubMed: 19011630]
10. Takada S, Kamiya R. Functional reconstitution of Chlamydomonas outer dynein arms from alpha-beta and gamma subunits: requirement of a third factor. The Journal of cell biology. 1994; 126:737–45. [PubMed: 8045937]
11. Koutoulis A, et al. The Chlamydomonas reinhardtii ODA3 gene encodes a protein of the outer dynein arm docking complex. The Journal of cell biology. 1997; 137:1069–80. [PubMed: 9166407]
12. Wirschell M, et al. Oda5p, a novel axonemal protein required for assembly of the outer dynein arm and an associated adenylate kinase. Molecular biology of the cell. 2004; 15:2729–41. [PubMed: 15064350]
13. Solnica-Krezel L, Schier AF, Driever W. Efficient recovery of ENU-induced mutations from the zebrafish germline. Genetics. 1994; 136:1401–20. [PubMed: 8013916]
14. Kimmel CB, Ballard WW, Kimmel SR, Ullmann B, Schilling TF. Stages of embryonic development of the zebrafish. Dev Dyn. 1995; 203:253–310. [PubMed: 8589427]
15. Rupp RA, Snider L, Weintraub H. Xenopus embryos regulate the nuclear localization of XMyoD. Genes Dev. 1994; 8:1311–23. [PubMed: 7926732]

16. Thisse, CaTB. High resolution whole-mount in situ hybridization. Zebrafish Science Monitor. 1998; 5:8–9.
17. Yelon D, Horne SA, Stainier DY. Restricted expression of cardiac myosin genes reveals regulated aspects of heart tube assembly in zebrafish. Dev Biol. 1999; 214:23–37. [PubMed: 10491254]
18. Milewski WM, Duguay SJ, Chan SJ, Steiner DF. Conservation of PDX-1 structure, function, and expression in zebrafish. Endocrinology. 1998; 139:1440–9. [PubMed: 9492081]
19. Tsukui T, et al. Multiple left-right asymmetry defects in Shh(−/−) mutant mice unveil a convergence of the shh and retinoic acid pathways in the control of Lefty-1. Proc Natl Acad Sci U S A. 1999; 96:11376–81. [PubMed: 10500184]
20. Yan YT, et al. Conserved requirement for EGF-CFC genes in vertebrate left-right axis formation. Genes Dev. 1999; 13:2527–37. [PubMed: 10521397]
21. Hellman NE, et al. The zebrafish foxj1a transcription factor regulates cilia function in response to injury and epithelial stretch. Proc Natl Acad Sci U S A. 2010; 107:18499–504. [PubMed: 20937855]
22. Panizzi JR, Jessen JR, Drummond IA, Solnica-Krezel L. New functions for a vertebrate Rho guanine nucleotide exchange factor in ciliated epithelia. Development. 2007; 134:921–31. [PubMed: 17267448]
23. Fliegauf M, et al. Mislocalization of DNAH5 and DNAH9 in respiratory cells from patients with primary ciliary dyskinesia. Am J Respir Crit Care Med. 2005; 171:1343–9. [PubMed: 15750039]
24. Drummond IA, et al. Early development of the zebrafish pronephros and analysis of mutations affecting pronephric function. Development. 1998; 125:4655–67. [PubMed: 9806915]
25. Becker-Heck A, et al. The coiled-coil domain containing protein CCDC40 is essential for motile cilia function and left-right axis formation. Nat Genet. 2011; 43:79–84. [PubMed: 21131974]
26. Kramer-Zucker AG, et al. Cilia-driven fluid flow in the zebrafish pronephros, brain and Kupffer's vesicle is required for normal organogenesis. Development. 2005; 132:1907–21. [PubMed: 15790966]
27. Witman GB. Isolation of Chlamydomonas flagella and flagellar axonemes. Methods in Enzymology. 1986; 134:280–290. [PubMed: 3821567]
28. King SM. Large-scale isolation of *Chlamydomonas* flagella. Methods Cell Biol. 1995; 47:9–12. [PubMed: 7476552]

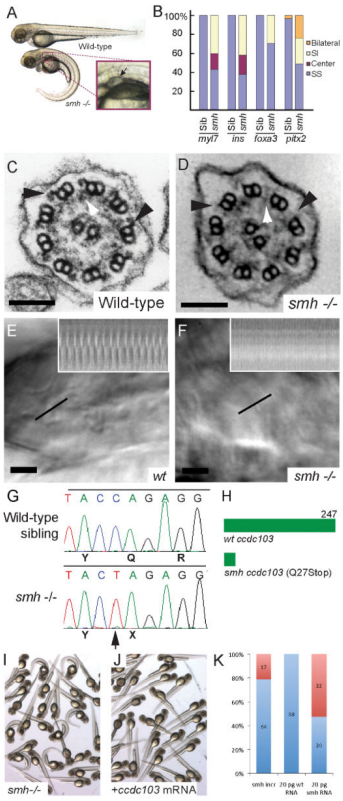


**Figure 1. The *schmalhans* mutation causes cilia paralysis and absent dynein arms**

**(A)** Wildtype sibling and *schmalhans* mutant embryos at 52 hpf with inset magnified view of *smh* pronephric cyst. **(B)** Quantification of *in situ* hybridization results showing left-right asymmetry defects in 48 hpf (*myl7*(*cmlc2*), *ins*, and *foxa3*) and 18 hpf (*pitx2*) *smh* embryos and siblings (sib). SI, Situs Inversus. SS, Situs Solitus. **(C–D)** Electron micrographs of cilia axonemes in a wild-type **(C)** and *smh* **(D)** pronephric duct. Outer dynein arms are highlighted by black arrowheads, inner dynein arms are indicated by white arrowheads. Scale bars in C and D = 100 nm. **(E–F)** Still images from wildtype (**E**; Supplementary Movie 1) and *schmalhans* mutant (**F**; Supplementary Movie 2) pronephric cilia showing position of line scan used to generate kymographs (insets in **(E)** and **(F)**). Scale bars in E and F = 5 μm. **(G)** Chromatogram showing the C to T change at base 79 in *ccdc103* resulting in Q to Stop at amino acid 27. **(H)** Schematic representation of the Ccdc103 proteins resulting from zebrafish (Dr) wild-type (WT) and *smh* (Q27Stop) coding sequence. **(I,J)** Rescue of axis curvature in a mutant clutch (**I**; white asterisks) by injection of 20 pg *ccdc103* synthetic mRNA (**J**). **(K)** Frequency of axis curvature defects in *smh* −/−, *smh* −/− + *ccdc103* mRNA, and *smh* −/− + Q27Stop *ccdc103* mutant mRNA demonstrates mutant rescue and partial dominant-negative effect of Q27Stop *smh ccdc103* mRNA. Red bars indicate the percent of embryos from an incross of *smh* heterozygotes that show the *smh* phenotype (Mendelian ~25% in uninjected embryos); blue bars indicate percent wild-type embryos; number of embryos in each class is indicated in the bars.


**Figure 2. Pedigrees of families carrying *CCDC103* loss of function mutations**

Pedigrees of the consanguineous families UCL-120, OP-1192 and OP-1193. Affected children are represented by black symbols; those with situs inversus are denoted with an asterisk (*). The affected individuals from all three families carry a homozygous loss-of-function mutation (c.383_384insG) predicting a premature stop of translation (p.Gly128fs25*). The parents (UCL-120I1 and I2, as well as OP-1193I1 and I2) are heterozygous carriers for the mutation. Segregation of the mutant allele is consistent with autosomal recessive inheritance.

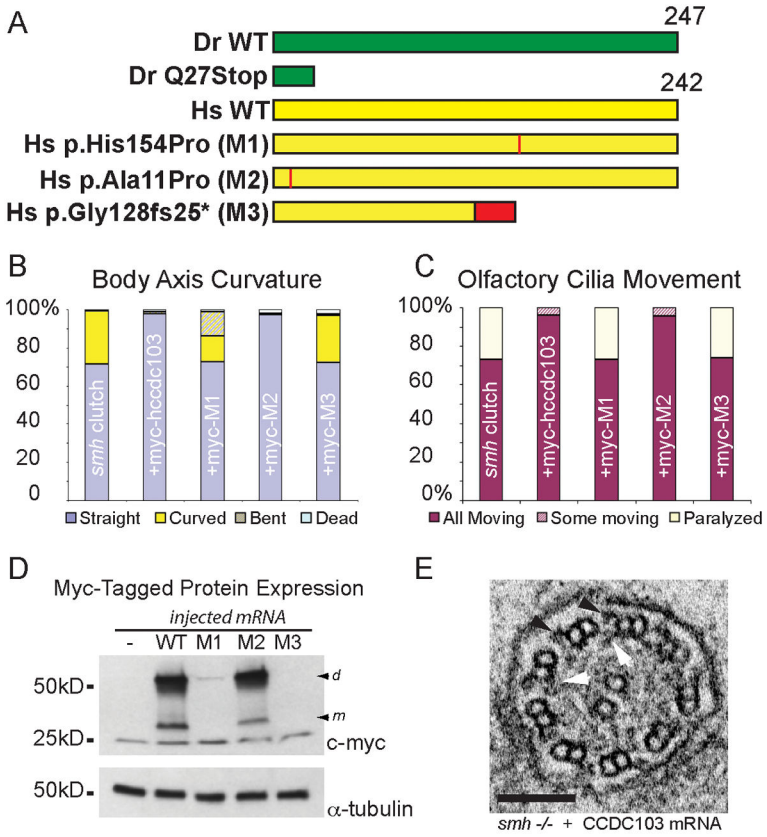


**Figure 3. Functional assay of human *CCDC103* mutant alleles in *smh* embryos**

**(A)** Graphical representation of zebrafish (green) and human (yellow) ccdc103 mutant alleles. Mutation position is noted in red. **(B)** Frequency of axis curvature observed in *smh* clutches alone, or injected with 35 pg synthetic RNA encoding the indicated form of human *CCDC103* at 36 hpf. *smh* clutches alone exhibited the expected 25% Mendelian ratio of affected homozygous mutants (yellow bar). **(C)** Frequency of cilia paralysis observed in *smh* clutches alone, or injected with 35 pg synthetic RNA encoding the indicated form of human *CCDC103* at 52 hpf. **(D)** Western blot detection of myc epitope-tagged Ccdc103 protein expression in 24 hpf whole-embryo extracts from *CCDC103* mRNA injected embryos (in **B** and **C**). *CCDC103* monomers (*m*) and dimers (*d*) are noted with arrowheads. Anti-alpha tubulin was used as a loading control. **(E)** Electron micrograph pronephric duct cilia from a 52 hpf *smh* −/− embryo that received injection of synthetic RNA encoding wildtype human Ccdc103. Outer dynein arms are marked with black arrowheads; white arrows mark inner dynein arms. Scale bar = 100 nm.

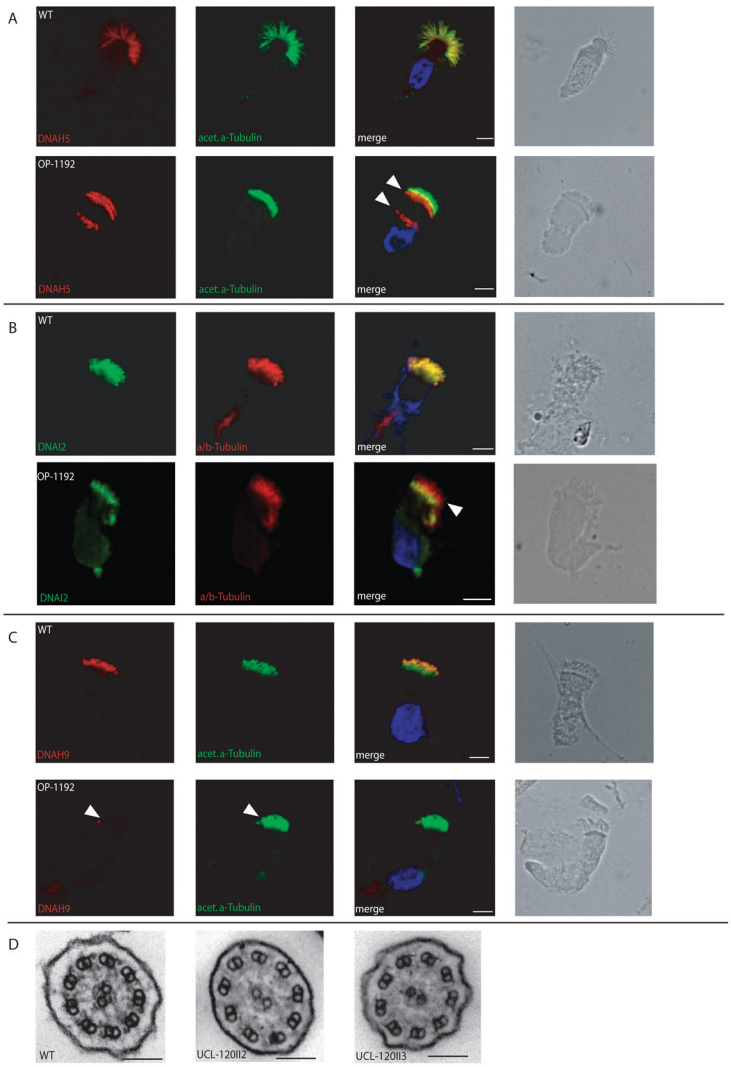


**Figure 4. Localization of DNAH5, DNAI2 and DNAH9 in respiratory epithelial cells from a PCD patient carrying the *CCDC103* loss-of-function mutation**

**(A–C)** Immunofluorescence analyses of human respiratory epithelial cells using specific antibodies directed against the outer dynein arm heavy chains DNAH5 **(A)** and DNAH9 **(C)** as well as the outer dynein arm intermediate chain DNAI2 **(B)**. As control, axoneme specific antibodies against acetylated α-tubulin **(A, C)** or α/β-tubulin **(B)** were used. Nuclei were stained with Hoechst 33342 (blue). **(A)** In respiratory epithelial cells from healthy probands, DNAH5 (red) localizes along the entire length of the axonemes. In respiratory epithelial cells from patient OP-1192 carrying the *CCDC103* loss-of-function mutation DNAH5 (red) localization is restricted to the proximal part of the axoneme and shows mis-localization to subapical cytoplasm and the perinuclear region (white arrowheads). **(B)** DNAI2 (green) is localized along the entire length of the axonemes of healthy probands. In contrast in respiratory cells of patient OP-1192 DNAI2 (green) localizes solely to the proximal ciliary axonemes (white arrowhead denotes cilia tips devoid of DNAI2 green fluorescence). **(C)** DNAH9 (red) localization is restricted to distal ciliary axonemes of respiratory epithelial cells from healthy probands, because it is only present in type2 ODA complexes. In the

patient OP-1192 DNAH9 is completely missing (white arrowhead) , consistent with altered assembly of type-2 ODA complexes. **(D)** Transmission electron microscopy of respiratory cilia showing normal outer- and inner-dynein arms in epithelial cells from a healthy proband. Respiratory cilia of two affected siblings carrying both identical homozygous CCDC103 loss-of-function mutations display variable defects of outer dynein arms. Cilia from patient UCL-120II2 display severe defects of the outer- and inner-dynein arms, whereas in cilia from the other affected sibling (UCL-120II3) seems to have remnant outer dynein arms. White scale bars **(A–C)** are 5μm. Black scale bars **(D)** are 0.1μm.

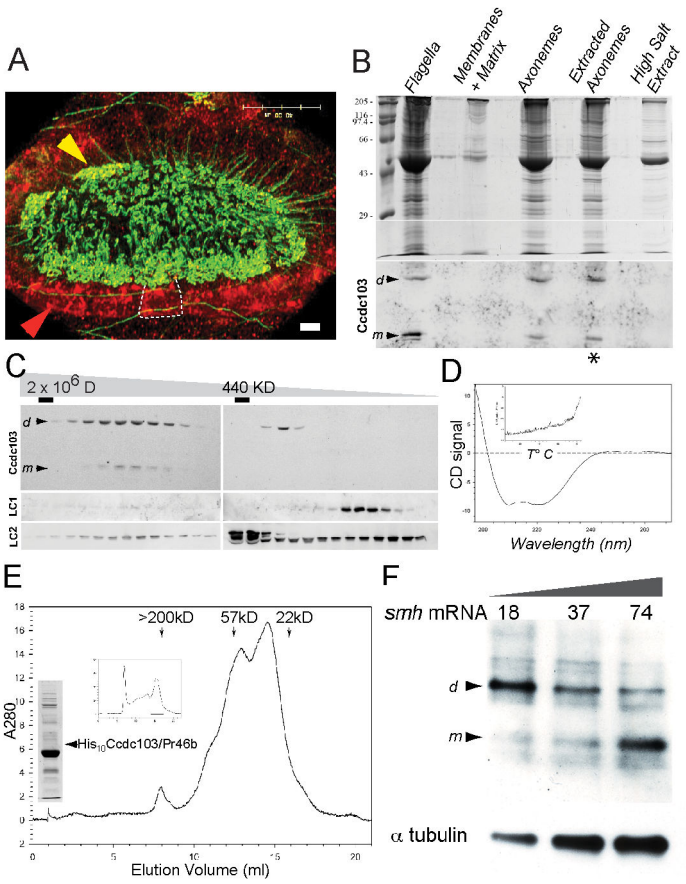


**Figure 5. Ccdc103 homodimers assemble with dynein light chain 2 in the cytoplasm and bind tightly to cilia axonemes**

**(A)** Ccdc103 (red) is expressed both in the cytoplasm (red arrowhead) and in anti-acetylated tubulin-positive (green) zebrafish olfactory placode cilia (yellow arrowhead) in 52 hpf zebrafish embryos. Dashed white line indicates the dimensions of a single olfactory placode multiciliated cell. Scale bar = 10 μm. See Supplementary Movie 7 for comparison live image of olfactory placode cilia. Ccdc103 staining was not observed in *smh* morpholino knockdown embryos (Supplementary figure 11). **(B)** Fractionation of *Chlamydomonas* flagella demonstrates Ccdc103/Pr46b is present in flagella and remains tightly associated with 0.6 M NaCl extracted axonemes (asterisk). Ccdc103/Pr46b migrates both as a monomer (*m*) and a dimer (*d*). **(C)** Ccdc103/Pr46b monomers (*m*) and dimers (*d*) co-purify with dynein light chain 2 (LC2) in a high molecular weight fraction (440,000 - 2,000,000 D, right panel) of Chlamydomonas cytoplasm and are also present in a lower molecular weight cytoplasmic fraction (<440,000 D, left panel). (**D**) Circular dichroism spectroscopic analysis of recombinant Ccdc103/Pr46b reveals strong alpha helical content and robust resistance to heat denaturation. (**E**) Gel filtration of recombinant Ccdc103/Pr46b demonstrates a mixture of dimer and monomer peaks. Single Gel lane (left) shows $Ni^{2+}$ column eluate containing recombinant His10-Ccdc103/Pr46b in total eluate protein. Pooled fractions from a superose 6 column (left chromatogram; black bar) fractionated on a Superdex 200 column (main chromatogram) revealed a mixture of monomer and dimer sized protein peaks. Western blotting for Ccdc103 confirmed Ccdc103 monomers and dimers in Superdex 200 fractions

(See Supplementary figure 16). (**F**) Mutant *smh*/Ccdc103 protein disrupts Ccdc103 dimer formation *in vivo*. Western blotting using anti-c-myc antisera to detect expression of myc-tagged full length zebrafish Ccdc103 mRNA (18 pg) when co-injected into wildtype embryos with increasing amounts (gradient indicated) of truncated *smh* Q27Stop protein. This revealed Ccdc103 dimers when co-expressed with low amounts of smh/Ccdc103 truncated protein (18 pg mRNA) but primarily monomers when co-expressed with high amounts of smh/Ccdc103 mRNA (74 pg). Anti-tubulin was used as a loading control.